

# Numerical Analysis of Continuous Dieless Wire Drawing Process

Rafid Jabbar Mohammed\*<sup>1</sup>, Jaafar Khalaf Ali<sup>2</sup>, Ameen Ahmed Nassar<sup>3</sup>

<sup>1,2,3</sup>Dept. of Mechanical Engineering, College of Engineering, University of Basrah, Basrah, Iraq

\*Corresponding Author Email: [rafidalsukaini@gmail.com](mailto:rafidalsukaini@gmail.com)

## Abstract

Dieless wire/tube drawing process is a novel technique has been developed in the past four decades utilizing super plasticity phenomenon, in which, the wire/tube is locally heated to a specified temperature and then subsequently locally cooled so as to further deformation is suppressed. This process is carried out without using the conventional drawing dies. A stainless steel SUS304 wire, 2mm diameter was used in this analysis. A coupled thermo-mechanical model has been developed and verified numerically. The thermal model was constructed to predict the temperature profile longitudinally along z-axis. As soon as the temperature distribution is obtained then the mechanical model was ready to predict the radius profile of the wire until the desired radius after deformation is satisfied. The effects of feeding velocity of the wire, heating coil length, cooling nozzle diameter, the distance between heating and cooling coils and radial distance which is affected by cooling air on temperature and radius profiles of the wire were considered here. Also, a symmetrical and asymmetrical distribution of the heat transfer coefficient for the wire cooling was also proposed in this study. The results showed that above parameters had important effects on temperature distribution and thus on radius profile of the drawn wire. Moreover, the symmetrical mode of heat transfer coefficient led to more stable for the temperature profile than asymmetrical mode. Consequently, to achieve more stability of this process, the above parameters must be determined accurately.

**Keywords:** Dieless wire drawing, Thermo-Mechanical Model, temperature distribution, radius profile.

## 1. Introduction

The Dieless wire drawing process was firstly presented by Alexander and Turner[1], they utilized SUS304 and Ti alloy bars and rods in the DLD process namely die-less drawing after that it is analyzed experimentally in detail by Sekiguchi et al.[2], who examined the drawability of pure titanium, SUS304, and carbon steel. Also, earliest, the dieless drawing process has been investigated experimentally by Hashmi et al. [3], who used the molten polymer to draw the copper wire of diameter 1.625mm. Furthermore, since 1969 the scientists utilized the concept of super plasticity to introduce the die-less drawing process as a novel technique instead of traditional drawing ways. They used Ti alloy and steels rods to investigate the DLD process abilities to achieve an area reduction of approximately 50%. The objective of DLD is reducing the cross-sectional area of a wire/tube without contact, where the elongation domain is situated between heating and cooling zone [4]. It is a flexible novel metal drawing technique has been developed without utilizing dies, which considers only the fact that the plastic flow stress of the metal decreases with increasing of deformation temperature [5]. Moreover, during plastic deformation in DLD, a grain refinement (in case of steel or any other microstructural transformation) was noticed [4].

The benefits of saving of materials, eliminating of friction forces, needless of pre-cleaning/lubricating of drawn materials, allowing for variable sections to be manufactured are advantages of DLD when compared with conventional processes. However, due to free deformation in the whole forming process, DLD has some

drawbacks than conventional drawing processes; instability and low deforming speed restrain its further development and application adversely [9].

There are three different kinds of DLD processes, namely Variants A, B, and C, as reported by Furushima et al. [6]. In type A and B, the heating/cooling units are moved and the wire is fixed at one side, whereas in type C, the heating/cooling units are fixed and the wire is moved i.e. it is continuous drawing process as illustrated in Fig.1.

Many investigations have been achieved to study the various parameters which effect on stability of DLD process theoretically and experimentally. Fann et al. [7] studied the evolution of temperature profile by suggesting a theoretical model for stainless steel SUS304 wire 5 mm diameter. Hwang et al. [8] conducted FE simulation along with experimental tests to study DLD critical parameters like temperature, drawing speed and area reduction and their effects on formability of stainless steel SUS304 tube 6.35 mm outer diameter. Tiernan et al. [10] and Huh et al. [15] studied the relationship between area reduction and final size variation. Their results proved that variation of final diameter increases with increasing of reduction ratio.

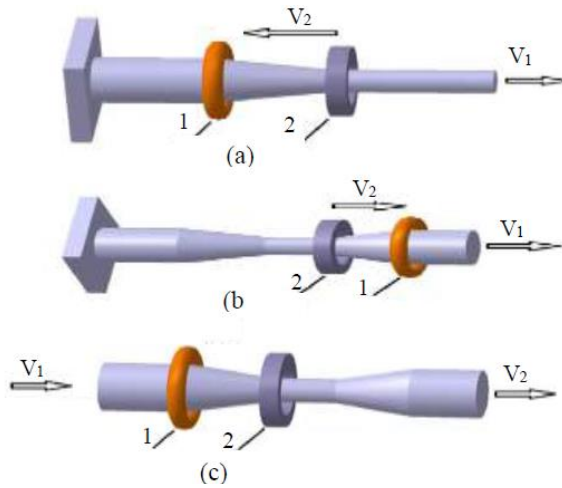


**Fig. 1:** The Variant Types of DLD Process, (a), (b) Non Continuous; (c) Continuous. 1-Heater; 2- Cooler [9]

Naughton et al. [11] investigated the stability of DLD process, where they concluded that stability of deformation process was well affected by feeding and drawing speeds, temperature distribution, heater-cooler units distance and reduction ratio. Hwang et al. [12] studied numerically and experimentally the effect of temperature profile on DLD of stainless steel tubes. Furushima et al. [13, 14] studied the thermal effect on deformation behavior in dieless tube drawing. They deduced that a steepest gradient of temperature is necessary to suppress the unstable deformation. Furushima et al. [16] carried out a finite element simulation to study the effect of path of drawing velocity on the deformation behavior.

Wang et al. [17] reported experimentally that tube wall thickness and wire diameter variation is affected by distance between heating and cooling units. Hongyu et al. [18] developed a novel theoretical model taking into account most of the DLD key parameters like drawing speeds, temperature states, material thermal properties.

In this paper, Variant (C) continuous dieless drawing—both heating and cooling coils are fixed and the wire is moved—will be depended. A thermo-mechanical model has been developed for SUS304 stainless steel wire with initial dia. of (1.6-2) mm to simulate temperature distribution through the longitudinal axis of the wire and to predict diameter profile.

## 1.1. Dieless Thermo-Mechanical Analysis

To implement the thermo-mechanical analysis, two models were used here, namely, heat transfer model and deformation model. Induction heating was used here as the heat supply method as recommended by many authors.

### 1.1.1. Heat Transfer Model

In this model, the heat conduction equation along with heat convection term equ.1 was solved numerically using central finite difference technique by MatLab code version R2017a. The following assumptions were considered in this model:

1. Temp. is assumed only a function of the longitudinal coordinate  $z$  along the wire.
2. The dieless drawing process is a steady axisymmetric process [21].
3. Electromagnetic field in the high frequency induction is not included.
4. Specific heat ( $C_p$ ), thermal conductivity ( $k$ ), and density ( $\rho$ ) are temperature independent. The material is isotropic.
5. The wire cross-sectional area is reduced during deformation process, but its effect on the temp. profile is negligible.
6. Steady State conditions after deformation are considered in this study

The balance of ingoing and outgoing heat per unit time of slice element is illustrated as in Fig.2: ( $ds$ : surface area,  $A$ : cross-section area,  $P$ : heat supply). From the energy balance of Fig.2, and by assuming a steady state condition the following governing equation where,  $\lambda=k/C_p\rho$  thermal diffusivity ( $m^2/s$ ) can be obtained:

$$\frac{d^2T}{dz^2} - \frac{V_0}{\lambda} \frac{dT}{dz} + \frac{2\pi R_0}{Ak} P - \frac{2\pi R_0 h}{Ak} (T - T_0) = 0 \quad (1)$$

The heat transfer model is illustrated by Fig. 3.

### 1.1.2. Boundary Conditions for HT Model

#### 1. Boundary Conditions for Heat Supply

The following boundary conditions were applied here, see Fig.3:

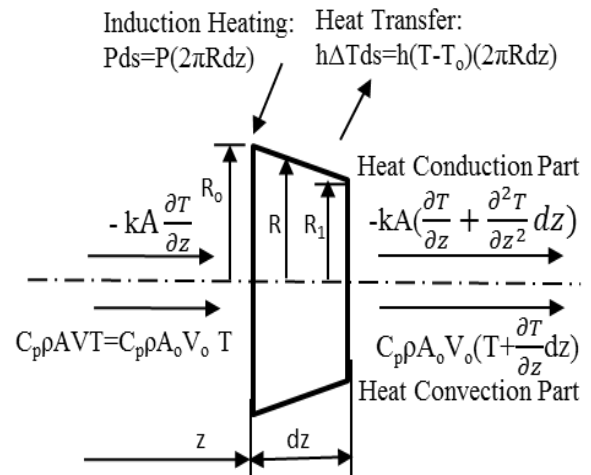


**Fig. 2:** Heat Balance in Heat Transfer Model

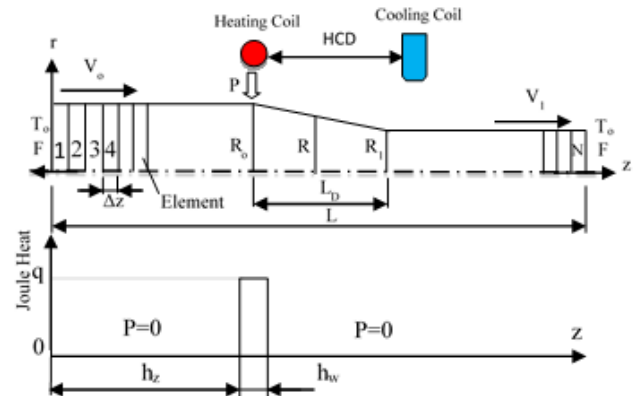


**Fig. 3:** Schematic of HT analysis Model

HCD: distance between heating and cooling coils,  $L$ : total length,  $L_D$ : deformation length,  $F$ : drawing force,  $T_0$ : ambient temp.,  $R_0$ : original radius,  $R_1$ : final radius,  $V_0$ : feeding velocity,  $V_1$ : drawing velocity,  $r$ : radial coordinate,  $z$ : longitudinal coordinate,  $h_z$ : location of heating coil,  $h_w$ : width of heating coil

$$a. T=T_0 \text{ at } z=0 \quad (2)$$

$$b. T=T_0 \text{ at } z=L \quad (3)$$

$$c. P=q \text{ at } h_z \leq z < (h_z + h_w) \quad (4)$$

$$d. P=0 \text{ at } (h_z + h_w) \leq z \leq h_z \quad (5)$$

where;  $P$  is quantity of heat supply per unit area ( $W/m^2$ ), and  $q$  is heat delivered from the heating induction coil to the wire surface.

2. Boundary Conditions for Heat Transfer Coefficient

In this model, Symmetric and asymmetric heat transfer distribution was proposed as explained in Fig.4.

1.1.3. Symmetric Trapezoid Shape

a. Heat transfer coefficient outside the cooling coil is specified as:

$$h = h_a \text{ at } (c_z + d_c + c_e) \leq z < (c_z - c_e) \quad (6)$$

b. Heat transfer coefficient outside the cooling coil but influence of cooling air is expanded :

$$h = \frac{(h_c - h_a)}{c_e} \{z - (c_z - c_e)\} + h_a \text{ at } c_z - c_e \leq z < c_z \quad (7)$$

$$h = \frac{(h_c - h_a)}{c_e} \{(c_z + d_c) - z\} + h_c \text{ at } c_z + d_c \leq z < c_z + d_c + c_e \quad (8)$$

c. Heat transfer coefficient directly under the cooling coil is allocated as:

$$h = h_c \text{ at } c_z \leq z < c_z + d_c \quad (9)$$

1.1.4. Asymmetric Trapezoid Shape

$$h = h_a \text{ at } (c_z + d_c + c_e) \leq z < c_z \quad (6a)$$

$$h = \frac{(h_c - h_a)}{c_e} \{(c_z + d_c) - z\} + h_c \text{ at } c_z + d_c \leq z < c_z + d_c + c_e \quad (8a)$$

$$h = h_c \text{ at } c_z \leq z < c_z + d_c \quad (9a)$$

The thermal properties of SUS304 Stainless Steel Wire is given in Table 1.

Table 1: Thermal Properties of SUS304 Wire [19]

Property	Value
Thermal Conductivity $k$ [W/(m.K)]	17
Specific Heat $C_p$ [J/(kg.K)]	500
Mass Density $\rho$ [kg/m <sup>3</sup> ]	8000
Thermal Diffusivity $\lambda$ [m <sup>2</sup> /s]	4.25E-6

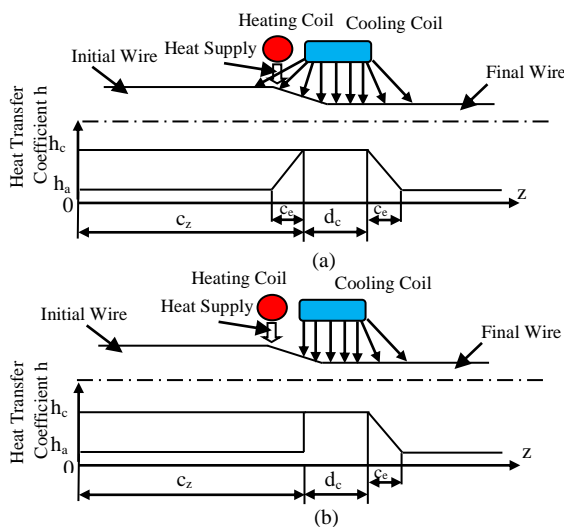


Fig. 4: Distribution of Heat Transfer Coefficient During Cooling Process in HT Model (a) symmetric trapezoid and (b) asymmetric trapezoid. Ce: distance which is affected by cooling air, Cz: location of cooling coil, dc: dia. of cooling nozzle.

2.2 Deformation Model

In superplastic flow, the flow stress is function of temperature, strain and strain rate [20], and used here to predict the radius profile. Following assumptions were considered:

1. Material is isotropic and incompressible.
2. One-dimensional stress profile (uniaxial loading)  $\sigma = \sigma(z)$  can be suggested.
3. Elasticity is negligible and the hypothesis of the plane cross-section is used, thus, the axial stress and velocity will do not change in the radial direction.
4. The drawing force  $F$  (force equilibrium condition) are invariant.
5. The material properties:  $K$  (coefficient of strength),  $n$  (exponent of strain hardening) and  $m$  (sensitivity index of strain rate) are temperature dependent.
6. Thermal strains are negligible in comparison with plastic strains.

The following power law for the plastic flow stress formula is often used to describe superplastic flow under uniaxial testing as the case in this study [20]:

$$\sigma = K(\epsilon_0 + \epsilon)^n (\dot{\epsilon}/\dot{\epsilon}_0)^m \quad (10)$$

$\epsilon_0$  is the initial strain and  $\dot{\epsilon}_0$  is a scaling factor, which is mostly assumed as  $1 \text{ s}^{-1}$ ,  $\epsilon_0$  : represents the offset strain which is approximately chosen to be equal to 0.01 to obviate zero stress state at zero strain [21]. The strain rate formula is given by:

$$\text{Strain rate equation: } \dot{\epsilon} = -2V_0 \frac{R_0^2}{R^3} \frac{dR}{dz} \quad (11)$$

And as mentioned earliest, that drawing force along the drawn wire is constant, that is

$$F = \sigma_0 A_0 = \sigma_1 A_1 = \sigma A = \text{const.} \quad (12)$$

$\sigma_0$  and  $\sigma_1$  : are elastic flow stress at initiating and ending stages of deformation.

$A_0$  and  $A_1$  : are area cross sections at initiating and ending stages of deformation.

$A$  : is cross sectional area at any arbitrary point within deformation zone.

$\sigma$  : is plastic flow stress at any arbitrary point within deformation zone.

Thus, from equations 10-12, the radius profile equation can be written as:

$$\frac{dR}{dz} = -\frac{R^3}{2V_0 R_0^2} \left\{ \frac{F}{K(\epsilon_0 + 2\ln \frac{R_0}{R})^n A} \right\}^{1/m} \quad (13)$$

Where;  $A = \pi R^2$

The reduction ratio of the cross section area is given by:

$$RA = \frac{A_0 - A_1}{A_0} = 1 - \frac{A_1}{A_0} \quad (14)$$

$$RA = 1 - \frac{V_0}{V_1} \quad (15)$$

2.2.1 Material Properties  $K, n, m$

The following equations for material properties  $K, n$  and  $m$  are used here [7]:

$$K(T) = 0.0007T^2 - 2.1417T + 1788.3 \quad (16)$$

$$n(T) = 4.645e-7T^2 - 3.628e-4T + 4.367e-1 \quad (17)$$

$$m(T) = 4.374e-5T + 1.449e-3 \quad (18)$$

2.2.2. Boundary Conditions for DF Model

To get equ.13 solved numerically for the radius profile, the following boundary conditions were applied as illustrated in Fig.5:

$$R = R_0 \text{ at } z = 0 \quad (19)$$

$$R=R_1 \text{ at } z=L \tag{20}$$

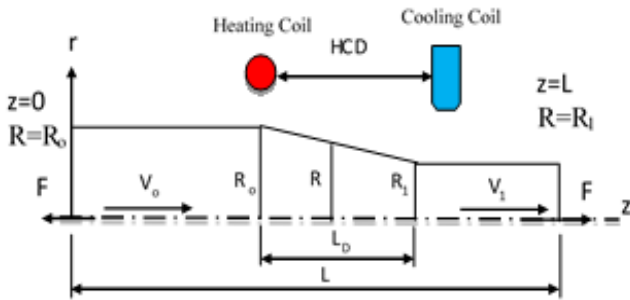


Fig. 5: Schematic of Deformation Model

Equ.13 was solved using three numerical approaches; 4<sup>th</sup> order Runge-Kutta, 5<sup>th</sup> order Runge-Kutta-Fehlberg and improved Euler methods with error of 1E-6.

### 3. Future Experimental Work

A comprehensive experimental tests is planned for the next study to validate the numerical analysis. Fig.6 explains designed machine by the author to simulate the dieless drawing process

### 4. Results and Discussion

#### 4.1. Effect of Feeding Velocity on Dieless Drawing Process

Effect of feeding velocity on temperature distribution is explained in Fig.7. It has been observed from this Fig. that max. temperature occurs nearly at 400 mm along longitudinal axis at the end of the heating coil for both symmetric and asymmetric mode. Also, was obvious that at low feeding velocity, the temperature gradient is steepest than at high velocities especially for symmetric mode, this is because of area which is affected by cooling air is larger than asymmetric case essentially towards the heating coil location. Consequently, the symmetric mode led to more stability for DLD process, where, the steepest gradient of temperature is the more steadiness of wire flow stress, this was also reported through studies carried out by Furushima and Tiernan. The stability of plastic flow stress after deformation effects principally on success of DLD process, since, after achieve area reduction within the deformation zone, then further deformation is prevented to happen. So, by providing an adequate cooling after deformation area directly, the flow stress will be increased significantly and additional deformation is halted. Effect of feeding velocity on flow stress in symmetric and asymmetric mode is presented in Fig.8. Visibly, symmetric mode had more effect on flow stress after deformation because of extended cooling distance.

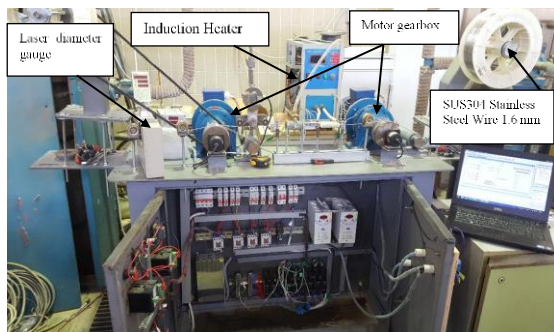


Fig. 6: Dieless wire drawing machine

Certainly, this will produce further stability of the DLD process and material grain refinement-since the grain size is depend on

heated region length and maximum temperature- which mean better mechanical properties as reported by the researchers. In general, increase of temperature will reduce the flow stress because of intensified dislocation motion within structure. Concurrently, low feeding velocity resulted lowest flow stress within deformation zone than high velocities, this is due to high quantity of heating delivered to the wire at low velocities. While DLD process utilizes the super plasticity phenomenon, the ranges of strain rate play a significant role in determine present or not of superplastic flow. As reported by many authors, the superplastic flow can be existed only at strain rates of  $(10^{-5} - 10^{-1} \text{ s}^{-1})$ , although super plasticity at high strain rates range  $1-10 \text{ s}^{-1}$  is also reported [20]. To achieve an invariant strain rate during the deformation process, the forming velocity should be increased, since with constant velocity during tensile test, the strain rate will be decreased. According to the volume constancy law, the velocity over the deformation zone is increased until reaching the final cross-section of area. It is very important to realize that high temperatures increase the ductility whilst high strain rates may have a negative effect on ductility. From Fig.9, it can be noted that maximum value of strain rate occurs at 400 mm end of heating coil and then decreases to the minimum value at end of deformation as the drawn wire is longer and temperature is lowest, which is agreed with [4], since lowest flow stress and highest strain rate occur at max. temperature region. Also, as seen from this Fig. that symmetric mode produced more stable strain rate with larger values than asymmetric, since symmetric cooling reduced the length of high-temperature zone and led to high level of strain rate, whilst, asymmetric cooling moved the deformation zone downstream towards cooling unit. Stability of final diameter with feeding velocity is plotted in Fig.10. At high velocities, the wire is not heated/cooled sufficiently and this effects on the flow stress of material and ductility.

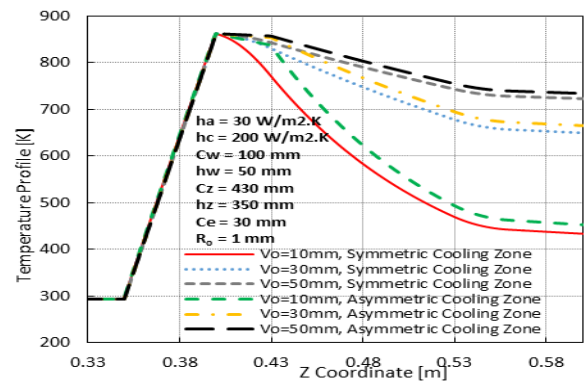


Fig. 7: Effect of Feeding Velocity on Temperature Profile

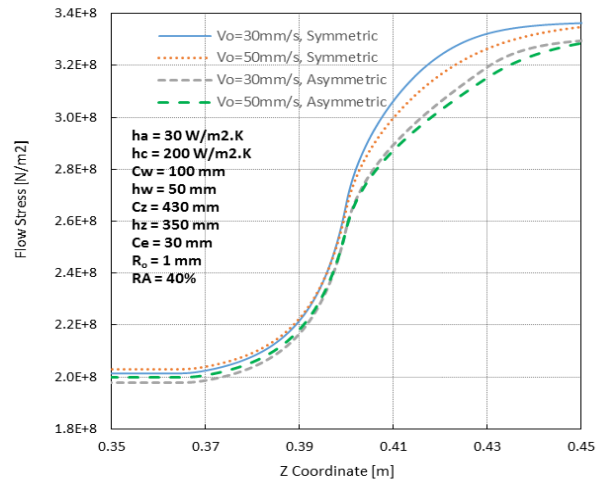


Fig. 8: Effect of Feeding Velocity on Flow Stress at Symmetric and Asymmetric Mode



### 4.2 Effect of Cw, hw, Ce and Cz on Dieless Drawing Process

Width of cooling coil (Cw) also had a significant effect on temperature profile as apparent from Fig.11, since, the high-temperature zone will be enlarged at small Cw especially for asymmetric mode, and more deformation may occur and poor strain hardening of the final product. Contrary, with increase of Cw, deformation zone will be reduced, further elongations are inhibited, good strain-hardening and more stability of the final diameter. Commonly, insufficient cooling leads to fracture and inadequate heating results to surface cracks. Effect of width of heating coil on temperature distribution is displayed in Fig.12. By increasing of heating coil width, the deformation zone will be extended in specific for asymmetric mode than symmetric mode, this was also reported by **Furushima and other authors**. Expansion of deformation zone may be unfavorable if further reduction is not required and may be more favorable if extra reduction is desired especially for fine wire/tube. To avoid fracture/cracks of the wire due to extra heating, either providing additional cooling or increasing the feeding speed.

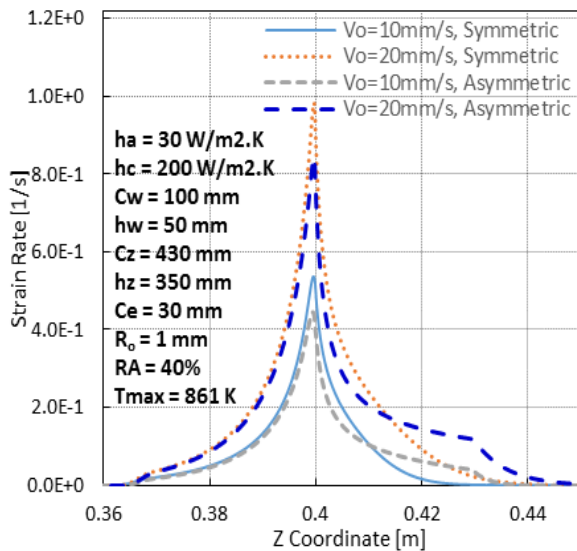


Fig. 9: Effect of Feeding Velocity on Strain Rate at Symmetric and Asymmetric Mode.

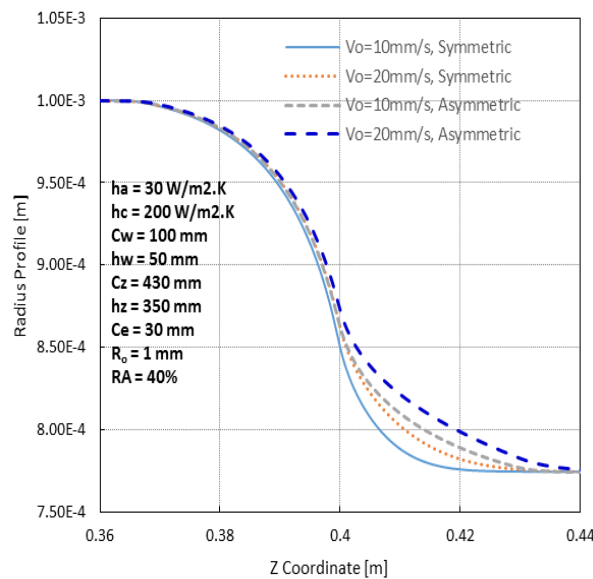


Fig. 10: Effect of Feeding Velocity on Radius Profile at Symmetric and Asymmetric Mode

But increasing of feeding velocity increases strain rate and may have adverse effects on ductility. So the temperature of the wire at deformation zone must be well controlled.

Effect of distance which is affected by cooling air (Ce) on wire temperature is explained in Fig.13. Clearly, increase (Ce) will reduce the length of deformation region particularly for symmetric mode and decrease the temperature by steepest manner because the wire will cool faster resulting in more stability of DLD process. Fig.14 displays the effect of location of cooling coil. By increasing (Cz), the deformation length will increase and more deformation will occur and the wire temperature will take more time to be dropped resulting in developing undesired thermal stresses.

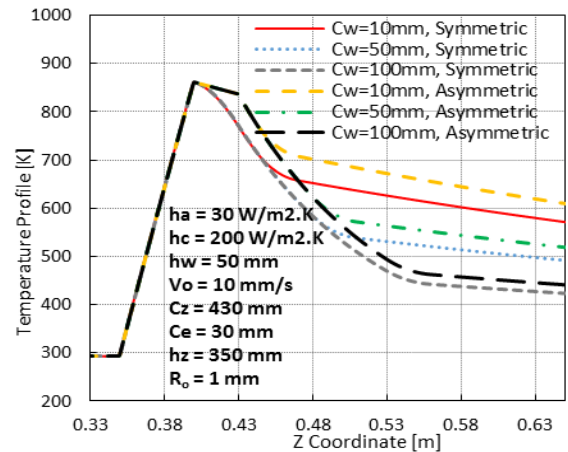


Fig. 11: Effect of Cooling Coil Width (Cw) on Temperature Profile at Symmetric and Asymmetric Cooling

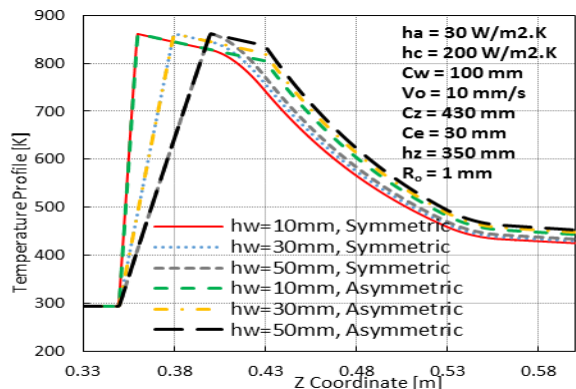


Fig. 12: Effect of heating Coil Width (hw) on Temperature Profile at Symmetric and Asymmetric Cooling

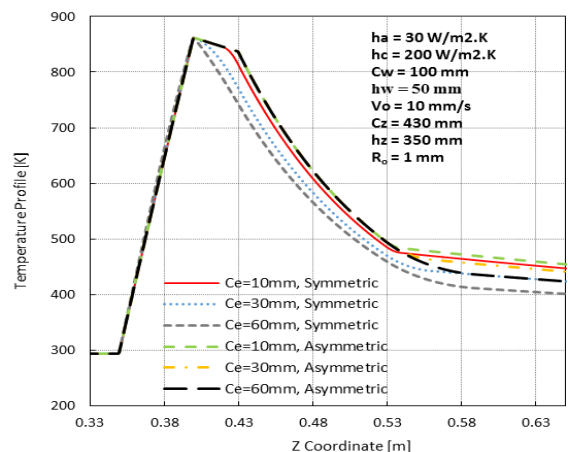


Fig. 13: Effect of Distance which is affected by cooling air (Ce) on Temperature Profile.

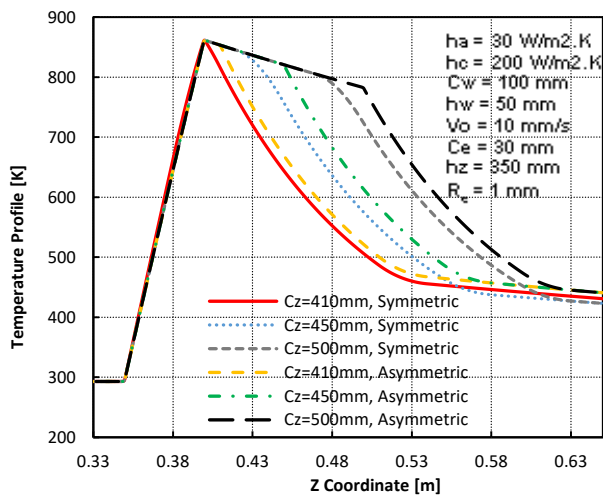


Fig. 14: Effect of Location of Cooling Coil (Cz) on Temperature Profile.

## 5. Conclusion

From the present study, the following remarks can be concluded:

- Feeding velocity ( $V_o$ ) had critical effects on temperature profile, strain rate and flow stress. So, it must be controlled well.
- Temperature must be controlled well within heating coil to reach the desired superplastic temperature ( $0.5T_m$ ). Also, adequate cooling must be delivered along deformation length, so temperature profile has steepest gradient.
- Flow stress is affected by  $V_o$ , where at high velocities, the wire will not be heated enough, so yielding point will not be reached earliest what effect on whole process.
- Max. strain rate will occur at end of heating process, and it is increased by increasing  $V_o$ , this may effect on ductility and may terminate the superplastic flow.
- Increase of cooling coil width ( $C_w$ ), will reduce the deformation zone and result in more control of temperature profile. Whereas, increasing ( $h_w$ ) will expand the deformation zone which is undesirable in some cases.
- Increasing ( $C_e$ ) led to softening deformation zone specifically for symmetric mode.
- Increasing ( $C_z$ ) had adverse effects on temperature profile, since it expanded the deformation zone and develop undesirable thermal stresses.
- Symmetric cooling mode had more active effect on stability of the process than asymmetric mode as explained beforehand.

## References

- T. W. Alexander, J. M. and Turner, "A preliminary investigation of the die-less drawing of titanium and some steels," *Proc. Mach. Tool Des. Res.*, vol. 15, pp. 525-537, 1974.
- K. Sekiguchi, H. Kobatake, and K. Osakada, "A fundamental study on dieless drawing," *Proc. Mach. Tool Des. Res.*, vol. 15, pp. 539-544, 1974.
- M. S. J. Hashmi, G. R. Symmons, and H. Parvinmehr, "A novel technique of wire drawing," *Arch. J. Mech. Eng. Sci.* 1959-1982 (vols 1-23), vol. 24, no. 1, pp. 1-4, 1982.
- F. M. R. Fortunier, H. Sassoulas, "A Thermo-Mechanical Analysis of Stability in Dieless Wire Drawing," *Int. J. Mech. Sci.*, vol. 39, no. 5, pp. 615-627, 1997.
- Z.T. Wang, G.F. Luan, G.R. Bai, "Study of the Deformation Velocity Field and Drawing Force During the Dieless Drawing of Tube," *Journal of Materials Processing Technology*, vol. 94, pp. 73-77, 1999.
- T. Furushima, K. Manabe, "Heat assisted dieless drawing process of superplastic metal microtubes-from Zn22Al to  $\beta$  titanium alloys," *Trans Tech Publications, Switzerland, Materials Science Forum*, vols. 838-839, pp. 459-467, 2016.
- K. J. Fann, C. F. Yu, C. H. Chang, "Analysis of dieless drawing to form the end of metal wires under proportional shape evolution with Slab method," *Trans Tech Publications, Switzerland, Materials Science Forum*, vol. 920, pp. 155-160, 2018.
- Y. M. Hwang, Z. S. Li, T. Y. Lin, "Formability Discussion in Dieless Drawing of Stainless Steel Tubes," *Trans Tech Publications, Switzerland, Key Engineering Materials*, vol. 626, pp. 10-15, 2015.
- Kai-Song Li, Xue-Feng Liu, Zhang-Zhi Shi, "Review of research status and development direction of dieless drawing," *Metall. Res. Technol.*, vol. 113, pp. 1-12, 2016.
- P. Tiernan, M.T. Hillery, "Experimental and numerical analysis of the deformation in mild steel wire during dieless drawing," *Journal of Materials: Design and Applications*, vol. 216, pp. 167-178, 2002.
- M.D. Naughton, P. Tiernan, "Requirements of a dieless wire drawing system," *Journal of Materials Processing Technology*, vol. 191, pp. 310-313, 2007.
- Y. Hwang, T. Kuo, "Dieless Drawing of Stainless Steel Tubes," *International Journal of Advanced Manufacturing Technology*, vol. 68, pp. 1311-1316, 2013.
- T. Furushima, K. Manabe, "FE analysis of size effect on deformation and heat transfer behavior in microtubedieless drawing," *Journal of Materials Processing Technology*, vol. 201, pp. 123-127, 2008.
- T. Furushima, T. Sakai, K. Manabe, "Finite element modeling of dieless tube drawing of strain rate sensitive material with coupled thermo-mechanical analysis," In: *Proceedings of the 8th International Conference on NUMIFORM*, pp. 522-527, 2004.
- Y. Huh, B.K. Ha, J.S. Kim, "Dieless drawing steel wires using a dielectric heating method and modeling the process dynamics," *Journal of Materials Processing Technology*, vol. 210, pp. 1702-1708, 2010.
- T. Furushima, S. Hirose, K. Manabe, "Effective Temperature Distribution and Drawing Speed Control for Stable Dieless Drawing Process of Metal Tubes," *Journal of Solid Mechanics and Materials Engineering*, vol. 3, no. 2, pp. 236-246, 2009.
- Z. T. Wang, S. H. Zhang, Y. Xu, G.F. Luan, G. R. Bai, "Experiment Study on the Variation of Wall Thickness During Dieless Drawing of Stainless Steel Tube," *Journal of Materials Processing Technology*, vol. 120, issues 1-3, pp. 90-93, 2002.
- W. Hongyu, J. Shijun, Z. Dewen, Z. Dianhua, "Analysis and study of dieless drawing process for rod based on radial direction gradient slab method," *The International Journal of Advanced Manufacturing Technology*, Springer-Verlag London Ltd., 2018.
- T. Furushima, T. Ikeda, Y. Noda, K. Manabe, "Deformation and Heat Transfer Analysis of Dieless Drawing Process for Metal Tube," *Steel Research Int. Special Edition*, pp. 302-307, 2011.
- K.A. Padmanabhan, R.A. Vasin, F.U. Enikeev, "Superplastic Flow: Phenomenology and Mechanics," *Springer-Verlag Berlin Heidelberg*, 2001.
- H. Jafari, "Thermo-Mechanical Investigation of Die-Less Wire Drawing Process," *MSc Thesis, University of British Columbia, Vancouver*, 2013.